

# Interfacial Misfit Array Technique for GaSb Growth on GaAs (001) Substrate by Molecular Beam Epitaxy

D. BENYAHIA,<sup>1,3</sup> Ł. KUBISZYN,<sup>2</sup> K. MICHALCZEWSKI,<sup>1</sup> A. KĘBŁOWSKI,<sup>2</sup>  
P. MARTYNIUK,<sup>1</sup> J. PIOTROWSKI,<sup>2</sup> and A. ROGALSKI<sup>1</sup>

1.—Institute of Applied Physics, Military University of Technology, 2 Kaliskiego Str., 00-908 Warsaw, Poland. 2.—Vigo System S.A., 129/133 Poznańska Str., 05-850 Ożarów Mazowiecki, Poland. 3.—e-mail: djalal.benyahia@wat.edu.pl

Undoped GaSb epilayers, deposited at low growth temperature (440°C), have been grown on GaAs (001) substrate with 2° offcut towards [110], by a molecular beam epitaxy system. Interfacial misfit array (IMF) growth mode has been used in order to impede the propagation of the threading dislocations through the GaSb epilayer. Under optimized growth parameters, both transmission electron microscopy (TEM) measurements and high-resolution x-ray diffraction (HRXRD) revealed the presence of a periodic array of pure 90° edge dislocations along [110]. Furthermore, HRXRD shows a full width at half maximum of a 2- $\mu\text{m}$ -thick GaSb epilayer peak as low as 195 arcsec. In addition, the GaSb layer is found to be 99.8% relaxed, with a residual strain of  $1.4 \times 10^{-4}$ . Moreover, based on TEM measurements, the dislocations spacing or the period of the IMF was found to be 5–5.2 nm.

**Key words:** Molecular beam epitaxy, GaSb, IMF, high-resolution x-ray diffraction, semiconductor III–V

## INTRODUCTION

Antimonide-based compound semiconductors have peculiar applications in a broad range of optoelectronic and electronic systems, thanks to their outstanding band alignments, small effective mass, and high electron mobility.<sup>1–3</sup> Hence, considerable attention has been given to these materials and use progress has been achieved in the devices' growth and invention; for instance, semiconductor lasers,<sup>4</sup> field effect transistors,<sup>5</sup> and infrared detectors.<sup>6</sup> Though recent developments have allowed the growth of high-quality lattice-matched GaSb epitaxy on native substrates, GaAs substrates are favored for many applications. This is due to their low cost, semi-insulating and suitable thermal properties, GaAs is transparent to more active regions, and it forms good *n* and *p* ohmic contact. However, the GaAs substrate and GaSb material exhibit a 7.8% lattice mismatch which results in a high

density of threading dislocations, typically on the order of  $10^9 \text{ cm}^{-2}$ .<sup>7</sup> This latter is highly detrimental to the electrical and optical properties of the device structures. Several techniques have been used to mitigate this deleterious effect, including metamorphic buffer layers,<sup>8</sup> strain-relief superlattice,<sup>9</sup> and interfacial misfit dislocation (IMF) growth mode.<sup>10</sup> In the metamorphic buffer layer approach, the strain is accommodated through tetragonal distortion in addition to defect formation, within a critical thickness. This technique shows several shortcomings, such as the indispensability to grow thick buffer layers (often  $> 1 \mu\text{m}$ ), poor thermal and electrical conductivity, and crucial material degradation through the formation of threading dislocations. In IMF growth mode, the strain is relieved instantaneously at the interface between the GaAs substrate and the GaSb epilayers by the formation of (2D) periodic IMF arrays consisting of pure-edge 90° dislocations along both [110] and [1-10] directions.<sup>11</sup> The growth of thick GaSb epilayers on GaAs substrates was considered to begin as islands and then merge to create layers, and in this

consideration, both  $60^\circ$  and  $90^\circ$  misfit dislocations exist.<sup>12</sup> However, the dominating strain relief mechanism was supposed to be  $90^\circ$  misfits, while the minority  $60^\circ$  ones were demonstrated to give birth to threading dislocations. The origin of the  $60^\circ$  misfits is still ambiguous, but it is believed to be related to three factors: island coalescence, the growth temperature, and the degree of the mismatch. Island coalescence has been demonstrated to cause  $60^\circ$  edge dislocations.<sup>10</sup> The growth temperature has been proved to be a robust factor in defining which misfit is formed: GaSb layers grown at  $\sim 520^\circ\text{C}$  favor  $90^\circ$  misfits, while at  $\sim 560^\circ\text{C}$  they favor  $60^\circ$  ones.<sup>13,14</sup> The lattice mismatch has been demonstrated to be a major factor in the formation of  $90^\circ$  misfits. Low strain ( $<2\%$ ) gives birth to  $60^\circ$  misfits, moderate strain ( $3\text{--}4\%$ ) results in mixed  $60^\circ$  and  $90^\circ$  misfits, and large strain ( $>6\%$ ) results in pure-edge  $90^\circ$  misfits.<sup>15</sup> There are some conflicts in IMF growth techniques across the literature. While all the recent groups confirm that the desorption of arsenic from the GaAs surface is the primary preoccupation, the option to switch from arsenic to antimony is performed at both the GaAs growth temperature and the GaSb growth temperature.<sup>16</sup> Transmission electron microscopy (TEM), etch pit density (EPD), and surface probe microscopy have been utilized to determine the threading dislocation density. However, these techniques have the disadvantage of being destructive methods. In addition, EPD measurements give an underestimation for dislocation densities greater than  $\sim 5 \times 10^6 \text{ cm}^{-2}$ .<sup>17</sup> Recently, non-destructive and large-area measurements have been performed by using x-ray diffraction (XRD) to analyze the threading dislocations formation.<sup>18–20</sup> These methods also have other advantages: the quantitative investigation such as the strain and the relaxation of GaSb epilayer on the GaAs substrate.

In this work, we report on the possibility to grow GaSb epilayers with the IMF approach on a GaAs (001) substrate at low growth temperature ( $440^\circ\text{C}$ ) in comparison to that reported by other groups ( $510^\circ\text{C}$ ).<sup>10</sup> The surface morphology has been assessed by Nomarski optical microscopy and high-resolution optical profilometry. In addition, cross-sectional TEM has been used to investigate the heterointerface GaAs/GaSb. The strain relaxation, dislocations density, and IMF properties have been characterized by high-resolution x-ray diffraction (HRXRD).

## EXPERIMENTAL

The samples have been grown on GaAs (001) substrates with  $2^\circ$  offcut towards [110] in a RIBER COMPACT 21-DZ solid-source molecular beam epitaxy system, equipped with valved crackers for As and Sb sources, and a BandiT system to monitor the substrate temperature. After thermal desorption of the oxide at  $600^\circ\text{C}$  under  $\text{As}_4$  overpressure, a 25-nm-

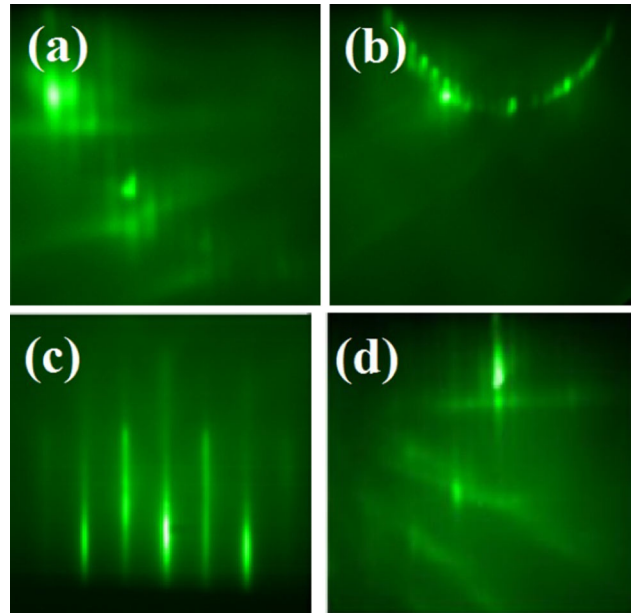


Fig. 1. GaSb layer RHEED patterns (a) ( $\times 4$ ) of the GaAs surface, (b) ( $\times 8$ ) of the Sb-soaked Ga-rich surface, (c) ( $\times 1$ ) of the GaSb surface (d) and ( $\times 3$ ) of the GaSb surface.

thick GaAs buffer layer was deposited at  $580^\circ\text{C}$  in order to get a smooth starting surface. The reflection high-energy electron diffraction (RHEED) pattern exhibits a  $2 \times 4$  (Fig. 1a) reconstruction indicating a flat As-rich surface.

For the growth of GaSb layers, after the GaAs deposition, the As and Ga shutters were closed to let the As adatoms desorb from the surface in order to have a Ga-rich surface. Theoretically, the RHEED pattern should change from  $2 \times 4$  to  $4 \times 2$ . In our growth, the  $2 \times 4$  pattern becomes faint, while the  $\times 2$  reconstruction transforms almost to a  $\times 3$  one. This Ga-rich surface is considered as the key for constituting highly periodic misfits. After waiting for about 30 min for the appearance of  $4 \times 2$ , the substrate temperature is cooled to  $440^\circ\text{C}$  under Sb overpressure. Interestingly, the RHEED pattern transforms to a  $2 \times 8$  reconstruction (Fig. 1b) revealing that the Sb adatoms have incorporated and the equilibrium state has been reached.<sup>21</sup> This reconstruction is proof of atomic packing instead of tetragonal distortion. Once the substrate temperature is stabilized at  $440^\circ\text{C}$ , the Ga beam flux is introduced, and the GaSb layer growth is initiated. Immediately, the RHEED exhibits a spotty pattern for the first few monolayers indicating a three-dimensional growth mode. During the growth of the next few monolayers, the RHEED shows a streaky  $1 \times 3$  pattern (Fig. 1c, d), which is evidence of a two-dimensional growth mode. Consequently, the GaSb growth is a Volmer–Weber growth mode. The growth rate for the GaSb layer was  $0.76 \mu\text{m/h}$  while the BEP (beam equivalent pressure) group V/III flux ratio (Sb/Ga) was set to be 5.

In order to protect the surface, the samples were cooled under Sb overpressure until 300°C, meanwhile the RHEED exhibits a  $1 \times 3$  pattern.

The structural quality and the defect properties of the grown samples were assessed by cross-sectional TEM. These measurements have been carried out on a FEI Talos microscope operating at 200 kV. Cross-sectional TEM specimens were got ready by a mechanical pre-thinning followed by an Ar ion milling. HRXRD of PANalytical X'Pert was used to investigate the crystallographic properties and the dislocation density in the GaSb layers. Furthermore, it was used to characterize the IMF array. The Cu  $K\alpha_1$  radiation ( $\lambda \approx 1.5406 \text{ \AA}$ ) originating from a line focus was used. The x-ray beam was monochromatized by a four-bounce Ge (004) hybrid monochromator. The measurements were performed in both the  $\omega$  and  $2\theta$ - $\omega$  directions. The in-plane measurements were performed in the [110] direction. On the other hand, the symmetric (004) and asymmetric (2-2-4) reciprocal space map (RSM) were performed. Surface morphology was assessed by Nomarski optical microscopy and high-resolution optical profilometry.

## RESULTS AND DISCUSSION

Figure 2 shows the surface morphology of undoped GaSb layers assessed by Nomarski optical microscopy. As can be seen, the surface of the grown sample was shiny mirror-like, under optimized growth conditions of growth temperature of 440°C and a Sb/Ga flux ratio of 5. A surface roughness as low as 3.3 nm was obtained under these conditions. On the other hand, the same surface quality was obtained under a group V/III flux ratio of 5 and at 250–540°C temperature range.<sup>22</sup> Rough surfaces ( $Rq = 145.2 \text{ nm}$ ), as can be noticed in Fig. 2b, were collected under a growth temperature of 420°C and a Sb/Ga flux ratio of 3.3.

The investigation of the interfacial misfit array using cross-sectional TEM image is shown in Fig. 3. This clearly shows the presence of a periodic array of misfit dislocations along [110]. The periodicity of the IMF array is measured to be 5–5.2 nm. The strain generated by the large lattice mismatch is relieved spontaneously by the formation of the IMF array at the interface. Analogous misfit dislocation periodicity was reported in GaSb growth on a GaAs substrate by Ref. 10. References 7 and 12 who proposed that the quasi-perfect relaxation of GaSb is effectively viable due to the high efficiency of the 90° misfits in the strain mismatch relieving.

The  $2\theta$ - $\omega$  scan of symmetric (004) and asymmetric (2-2-4) HRXRD spectra for a 2- $\mu\text{m}$ -thick GaSb layer grown using IMF technique are shown in Fig. 4a and b, respectively. The position of the GaSb layers depends on the reflection and the strain between the layer and the GaAs substrate. The peak separation between the GaAs substrate and the GaSb layers could be solely determined to be 9590 arcsec, which

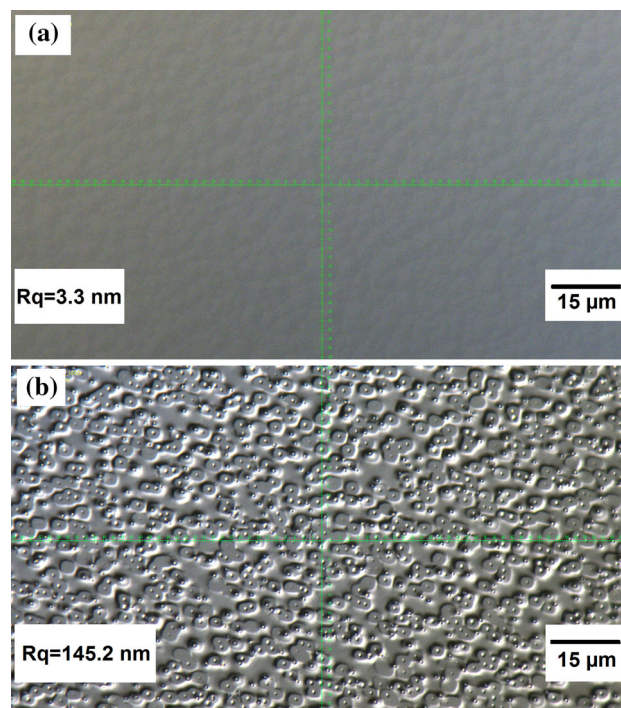


Fig. 2. The Nomarski optical microscopy pictures with a magnification of  $\times 1000$  of a 2- $\mu\text{m}$ -thick GaSb layer grown (a) under optimized parameters and (b) under unoptimized parameters.

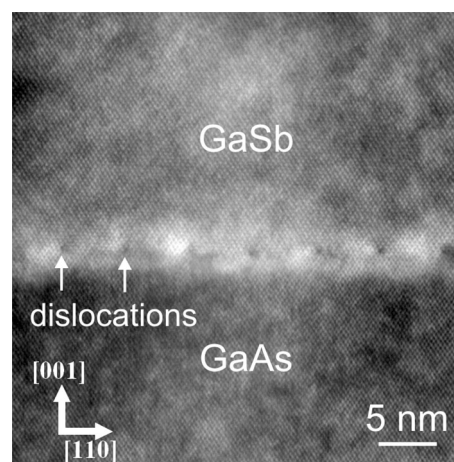


Fig. 3. Cross-sectional TEM imaging of GaSb epilayers grown on a GaAs substrate.

corresponds to the theoretical value of a relaxed GaSb layer (9554 arcsec). During the cooling of the substrate temperature, after the growth of the GaSb layer, the cubic structure can be distorted to a tetragonal one. The perpendicular lattice parameter “ $c$ ”, and the parallel one “ $a$ ”, to the GaAs/GaSb interface, have been calculated from the  $2\theta$ - $\omega$  scans for symmetric (004) and asymmetric (2-2-4) reflections, respectively (Fig. 4), using the followings equations:

$$c = 2\lambda / \sin(\theta_{004}) \quad (1)$$

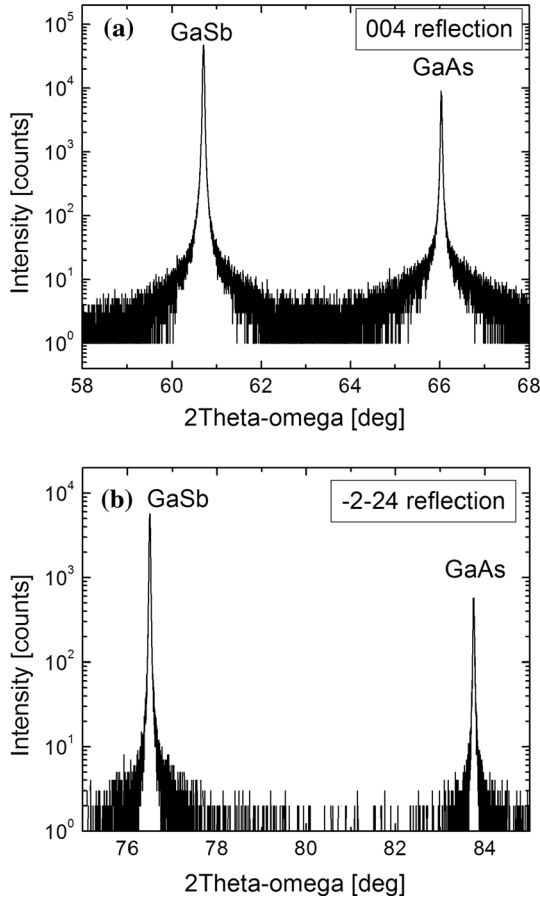


Fig. 4. HRXRD  $2\theta$ - $\omega$  scans for the GaSb layer grown on a GaAs substrate for (a) symmetric (004) reflection and (b) asymmetric (2-2-4) reflection.

$$\frac{1}{d_{hkl}^2} = \frac{h^2 + k^2}{a^2} + \frac{l^2}{c^2} \quad (2)$$

where  $\lambda$  is the wavelength of the x-ray beam,  $d_{hkl}$  is the spacing between the planes ( $hkl$ ), here ( $hkl$ ) = (2-2-4). While the relaxed lattice parameter has been calculated from the following equation:

$$a_{\text{relax}} = (c + 2ba)/(1 + 2b) \quad (3)$$

where  $b = (1 - \nu)/(1 + \nu)$ , and  $\nu$  is the Poisson ratio determined by  $\nu = C_{12}/(C_{11} + C_{12})$ , where the elastic stiffness parameters  $C_{11} = 8.85 \times 10^{10} \text{ N/m}^2$  and  $C_{12} = 4.04 \times 10^{10} \text{ N/m}^2$ .<sup>23</sup>

The in-plane lattice parameter “ $a$ ” is determined to be 6.0942 Å, while the perpendicular one is 6.0959 Å. On the other hand, the relaxed lattice parameter is 6.0950 Å. The relaxation, which is defined by Eq. 4, is found to be 99.8%.

$$R = (a - a_{\text{subst}})/(a_{\text{relax}} - a_{\text{subst}}) \quad (4)$$

GaSb layers grown on a GaAs substrate undergo biaxial compressive strain because of the lattice mismatch, and a tensile strain due to the difference

in thermal expansion coefficient between GaSb ( $7.75 \times 10^{-6} \text{ K}^{-1}$ ) and GaAs ( $5.7 \times 10^{-6} \text{ K}^{-1}$ ).<sup>24,25</sup> Generally, the strain generated by the lattice mismatch is quickly relieved through the formation of misfit dislocations. The residual strain is the consequence of the difference between the thermal expansion coefficients of the epilayer and the substrate. Vertical strain  $\varepsilon$  in the GaSb layers is determined to be  $1.4 \times 10^{-4}$  by the following equation:

$$\varepsilon = (c - a_{\text{relax}})/a_{\text{relax}} \quad (5)$$

The dislocations in the single-crystal semiconductor causes the broadening of the rocking curve in two ways: (1) it introduces a rotation of the crystal lattice, which immediately broadens the rocking curve; and (2) these dislocations are encircled by a strain field, in which the Bragg angle of the crystal is not uniform.<sup>18</sup> The dislocations density ( $D$ ) can be calculated from rotational broadening (Eq. 6) and from the strain broadening (Eq. 7) as follows<sup>18</sup>:

$$D = K_x/4.36b^2 \quad (6)$$

$$D = K_\varepsilon/0.090b^2 \left| \ln \left( 2 \times 10^{-7} \text{ cm} \sqrt{D} \right) \right| \quad (7)$$

where  $b$  is the Burger’s vector, in our case,  $b = a/2$ .<sup>10</sup> While  $K_x$  and  $K_\varepsilon$  are two parameters determined from the following equation:

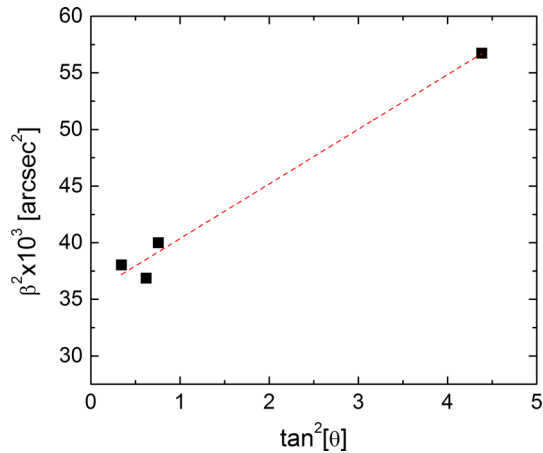
$$\beta^2 = K_x + K_\varepsilon \tan^2 \theta \quad (8)$$

where  $\beta$  is the measured full width at half maximum (FWHM) of the GaSb epilayer. Four rocking curves were performed at different values of  $\theta$  (Table I). Having plotted  $\beta^2$  as a function of  $\tan^2 \theta$ , the parameters  $K_x$  and  $K_\varepsilon$  are determined from the intercept and the slope (Fig. 5), respectively. One can readily calculate  $K_x$  and  $K_\varepsilon$  to be 32,568 arcsec<sup>2</sup> and 5184 arcsec<sup>2</sup>, respectively. Thus, the dislocations density determined from the rotational broadening is  $1.89 \times 10^8 \text{ cm}^{-2}$ , while based on the strain broadening,  $D$  is equal to  $2.53 \times 10^8 \text{ cm}^{-2}$ , which is in suitable agreement with the previous result. This agreement confirms the presence of 90° misfit dislocations.<sup>18</sup> In the existence of 60° misfit dislocations, the threading dislocation density determined by the strain broadening is reduced by a factor of two compared to that calculated from the rotational broadening. Reference 10 have reported a dislocation density of  $\sim 10^5 \text{ cm}^{-2}$ .

The dislocation type can be identified by two parameters: the angle  $\phi$  of the 2-2-4 RSM and the FWHM ratio for both the symmetric and rocking curves of the 004 reciprocal lattice point (RLP).<sup>26</sup> Figure 6 exhibits the RSM of the GaSb layers for the 004 and 2-2-4 reflections. The first RSM is used to calculate the GaSb 004 FWHM ratio between  $Q_z$  and  $Q_x$  directions, while the second one is required to determine the angle  $\phi$  between the FWHM and the

**Table 1. X-ray rocking curve data for a 2- $\mu\text{m}$ -thick GaSb layer grown on a GaAs substrate using the IMF technique**

$(hkl)$	$\theta, ^\circ$	$\text{Tang}^2\theta$	$\beta, \text{arcsec}$
(004)	30.38	0.34	195
(115)	41.02	0.76	200
(117)	64.47	4.38	238
(2-2-4)	38.24	0.79	192


 Fig. 5. The  $\beta^2$  versus  $\tan^2\theta$  for a 2- $\mu\text{m}$ -thick GaSb layer grown on a GaAs substrate.

$Q_x$  direction. The expected value of  $\phi$  can approach  $38^\circ$  for the  $90^\circ$  misfits dislocation, and  $36^\circ$  in the presence of  $60^\circ$  dislocations. The 2-2-4 RSM plotted in Fig. 6b revealed a value of  $41.0^\circ$  for the angle  $\phi$ . On the other hand, the FWHM ratio is believed to be 0.37 for  $60^\circ$  edge dislocations and 0.71 for the  $90^\circ$  ones. From Fig. 6a, this ratio is found to be 0.30. Reference 20 demonstrates that both parameters  $\phi$  and FWHM ratio are thickness-dependent. For instance, the angle  $\phi$  shifts from  $33^\circ$  to  $37^\circ$  (FWHM ratio increase from 0.4 to 0.55), when the GaSb thickness increases from  $0.25 \mu\text{m}$  to  $1.5 \mu\text{m}$ . The precedent utilization of this method (especially GaAs on Si) were in the case of a thick buffer layer which were more probably completely relaxed.<sup>27</sup> The superelliptical shape of the asymmetric RSM shown in Fig. 6b gives ample proof that the IMF array of the  $90^\circ$  edge dislocations is formed.<sup>26</sup>

Reference 26 report on a simple method to characterize a correlated dislocations array. The relationship between misfit dislocations is as follow:

$$\Delta Q = K \sqrt{\gamma \rho / d} \quad (9)$$

where  $\Delta Q$  is the scattering vector,  $d$  is the thickness of the GaSb layer,  $\rho$  is the dislocation line density,  $\gamma$  is the correlation factor, and  $K$  is a parameter determined by the scan direction in reciprocal

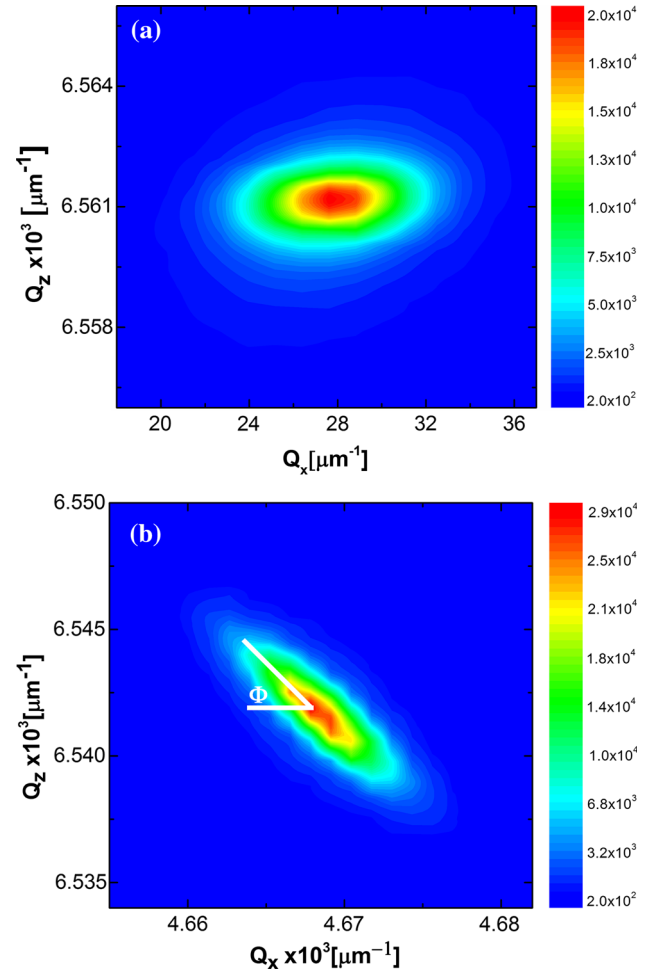


Fig. 6. RSM of GaSb layers grown on a GaAs substrate for (a) symmetric 004 reflection and (b) asymmetric 2-2-4 reflection.

space, the dislocation type, and the RLP.<sup>26,28</sup> For GaSb layers grown on the GaAs substrate, the  $K$  parameter is 11.805 for  $\Delta Q_x$  and 8.347 for  $\Delta Q_z$ .<sup>29</sup> Moreover, the correlation factor  $\gamma$  is equal to 0.015 for  $\Delta Q_x$  and 0.005 for  $\Delta Q_z$ .<sup>20</sup> Thus, the dislocations line density is  $0.1495 \text{ nm}^{-1}$ , which leads to a dislocations spacing of 6.7 nm. This is greater than that measured by TEM (which is the accurate value), and we believe that this difference is within the experiment error.

## SUMMARY AND CONCLUSIONS

In summary, high-quality GaSb epilayers have been grown on a GaAs (001) substrate using the MF approach. This growth was performed at low growth temperature compared to that reported in the literature. A mirror-like surface was obtained with a roughness of 3 nm. The presence of the MF array of 90° pure-edge dislocations along [110] was confirmed by TEM measurements with a periodic spacing of 5–5.2 nm. On the other hand, the IMF presence is also confirmed by HRXRD analysis. The GaSb layers have been found to be 99.8% relaxed, with a residual strain of  $\sim 10^{-4}$ . The dislocations density was determined to be as low as  $10^{-8} \text{ cm}^{-2}$ . Future work should look to decreasing dislocations density.

## ACKNOWLEDGEMENT

This paper has been completed with the financial support of the Polish National Science Centre, Project: UMO-2015/17/B/ST5/01753.

## OPEN ACCESS

This article is distributed under the terms of the Creative Commons Attribution 4.0 International License (<http://creativecommons.org/licenses/by/4.0/>), which permits unrestricted use, distribution, and reproduction in any medium, provided you give appropriate credit to the original author(s) and the source, provide a link to the Creative Commons license, and indicate if changes were made.

## REFERENCES

1. R.A. Hogg, K. Suzuki, K. Tachibana, L. Finger, K. Hirakawa, and Y. Arakawa, *Appl. Phys. Lett.* 72, 2856 (1998).
2. L. Müller-Kirsch, R. Heitz, U.W. Pohl, D. Bimberg, I. Häussler, H. Kirmse, and W. Neumann, *Appl. Phys. Lett.* 79, 1027 (2001).
3. Y.B. Li, Y. Zhang, and Y.P. Zeng, *J. Appl. Phys.* 109, 073703 (2011).
4. O. Cathabard, R. Teissier, J. Devenson, J.C. Moreno, and A.N. Baranov, *Appl. Phys. Lett.* 96, 141110 (2010).
5. H.K. Lin, D.W. Fana, Y.C. Lina, P.C. Chiua, C.Y. Chiena, P.W. Lia, J.I. Chyia, C.H. Kob, T.M. Kuanb, M.K. Hsiehb, W.C. Leeb, and C.H. Wann, *Solid State Electron.* 54, 505 (2010).
6. E.H. Aifer, J.G. Tischler, J.H. Warner, I. Vurgaftman, W.W. Bewley, J.R. Meyer, J.C. Kim, L.J. Whitman, C.L. Canedy, and E.M. Jackson, *Appl. Phys. Lett.* 89, 053519 (2006).
7. A. Rocher, *Solid State Phenom* 19/20, 563 (1991).
8. J.W. Matthews and A.E. Blakeslee, *J. Cryst. Growth* 29, 131911 (1975).
9. B.R. Bennett, *Appl. Phys. Lett.* 73, 3736 (1998).
10. S.H. Huang, G. Balakrishnan, A. Khoshakhlagh, A. Jallipalli, L.R. Dawson, and D.L. Huffaker, *Appl. Phys. Lett.* 88, 131911 (2006).
11. A. Jallipalli, G. Balakrishnan, S.H. Huang, T.J. Rotter, K. Nunna, B.L. Liang, L.R. Dawson, and D.L. Huffaker, *Nanoscale Res. Lett.* 4, 1458 (2009).
12. W. Qian, M. Skowronski, R. Kaspi, M. De Graef, and V.P. David, *J. Appl. Phys.* 81, 7268 (1997).
13. J.-H. Kim, T.-Y. Seong, N.J. Mason, and P.J. Walker, *J. Electron. Mater.* 27, 466 (1998).
14. W. Qian, M. Skowronski, and R. Kaspi, *J. Electrochem. Soc.* 144, 1430 (1997).
15. R.E. Mallard, P.R. Wilshaw, N.J. Mason, P.J. Walker, and G.R. Booker, *Microsc. Semiconduct. Matter.* 100, 331 (1989).
16. C.J.K. Richardson, L. He, and S. Kanakaraju, *J. Vac. Sci. Technol. B* 29, 03C126 (2011).
17. D.J. Stirland, *Appl. Phys. Lett.* 53, 2432 (1988).
18. J.E. Ayers, *J. Cryst. Growth* 135, 71 (1994).
19. A. Yu Babkevich, R.A. Cowley, N.J. Mason, S. Weller, and A. Stunault, *J. Phys.: Condens. Matter* 14, 13505 (2002).
20. C.J. Reyner, J. Wang, K. Nunna, A. Lin, B. Liang, M.S. Goorsky, and D.L. Huffaker, *Appl. Phys. Lett.* 99, 231906 (2011).
21. F. Maeda and Y. Watanabe, *Phys. Rev. B* 60, 10652 (1999).
22. D. Benyahia, L. Kubiszyn, K. Michalczewski, A. Kębłowski, P. Martyniuk, J. Piotrowski, and A. Rogalski, *Opto-Electron. Rev.* 24, 40 (2016).
23. J.E. Ayers, *Heteroepitaxy of Semiconductors: Theory, Growth, and Characterization* (Boca Raton: Taylor & Francis Group, LLC, 2007), p. 25.
24. P.S. Dutta, H.L. Bhat, and V. Kumar, *J. Appl. Phys.* 81, 5821 (1997).
25. H. Tatsuoka, H. Kuwabara, H. Fujiyasu, and Y. Nakanishi, *J. Appl. Phys.* 65, 2073 (1989).
26. V.M. Kaganer, R. Köhler, M. Schmidbauer, R. Opitz, and B. Jenichen, *Phys. Rev. B* 55, 1793 (1997).
27. V.M. Kaganer, A. Shalimov, J. Bak-Misiuk, and K.H. Ploog, *Appl. Phys. Lett.* 89, 021922 (2006).
28. A. Shalimov, J. Bak-Misiuk, V.M. Kaganer, M. Calamitout, and A. Georgakilas, *J. Appl. Phys.* 101, 013517 (2007).
29. A. Bourret and P.H. Fuoss, *Appl. Phys. Lett.* 61, 9 (1992).